A Cluster of Mutations in the UMOD Gene Causes Familial Juvenile Hyperuricemic Nephropathy with Abnormal Expression of Uromodulin

KARIN DAHAN,* OLIVIER DEVUYST,† MICHÈLE SMAERS,* DIDIER VERTOMMEN,† GUY LOUTE,§ JEAN-MICHEL POUX,‖ BÉATRICE VIRON,¶ CHRISTIAN JACQUOT,# MARIE-FRANCE GAGNADOUX,** DOMINIQUE CHAUVEAU,†† MATHIAS BÜCHLER,‡‡ PIERRE COCHAT,§§ JEAN-PIERRE COSYNS,‖‖ BÉATRICE MOUGENOT,¶¶ MARK H. RIDER,‡ CORINNE ANTIGNAC,## CHRISTINE VERELLEN-DUMOULIN*, and YVES PIRSON†

**Université Catholique de Louvain, Center for Human Genetics, Brussels, Belgium; †Université Catholique de Louvain, Division of Nephrology, Brussels, Belgium; ‡Université Catholique de Louvain, International Institute of Cellular and Molecular Pathology, HORM Unit, Brussels, Belgium; §Hôpital Princesse Paola, Department of Nephrology, Aye, Belgium; ‖Hôpital de Frejus, Department of Nephrology, Frejus, France; ¶Hôpital Bichat-Claude Bernard, Department of Nephrology, Paris, France; #Hôpital Georges Pompidou, Department of Nephrology, Paris, France; **Hôpital Necker, Department of Pediatric Nephrology, Paris, France; ††Hôpital Necker, Department of Nephrology and INSERM U507, Paris, France; ‡‡Centre Hospitalier Régional, Department of Nephrology, Tours, France; §§Hôpital Edouard Herriot, Department of Pediatric Nephrology, Lyon, France; ‖‖Université Catholique de Louvain, Department of Pathology, Brussels, Belgium; ¶¶Hôpital Tenon, Department of Pathology, Paris, France; and ##Université Paris V, Necker Hospital, INSERM U574, and Department of Genetics, Paris, France*

Abstract. Familial juvenile hyperuricemic nephropathy (FJHN [MIM 162000]) is an autosomal-dominant disorder characterized by abnormal tubular handling of urate and late development of chronic interstitial nephritis leading to progressive renal failure. A locus for FJHN was previously identified on chromosome 16p12 close to the *MCKD2* locus, which is responsible for a variety of autosomal-dominant medullary cystic kidney disease (MCKD2). *UMOD*, the gene encoding the Tamm-Horsfall/uromodulin protein, maps within the *FJHN/MCKD2* critical region. Mutations in *UMOD* were recently reported in nine families with FJHN/MCKD2 disease. A mutation in *UMOD* has been identified in 11 FJHN families (10 missense and one in-frame deletion)—10 of which are novel—clustering in the highly conserved exon 4. The consequences of *UMOD* mutations on uromodulin expression were investigated in urine samples and renal biopsies from nine patients in four families. There was a markedly increased expression of uromodulin in a cluster of tubule profiles, suggesting an accumulation of the protein in tubular cells. Consistent with this observation, urinary excretion of wild-type uromodulin was significantly decreased. The latter findings were not observed in patients with FJHN without *UMOD* mutations. In conclusion, this study points to a mutation clustering in exon 4 of *UMOD* as a major genetic defect in FJHN. Mutations in *UMOD* may critically affect the function of uromodulin, resulting in abnormal accumulation within tubular cells and reduced urinary excretion.

Familial juvenile hyperuricemic nephropathy (FJHN) is an autosomal-dominant disorder characterized by hyperuricemia and decreased urinary excretion of urate, followed by the development of chronic interstitial nephritis most often leading to progressive renal failure (1,2). The link between early hyperuricemia and subsequent progression of renal disease remains unclear.

Urate is the end product of purine metabolism in humans, who have lost the expression of the uricase gene during evolution (3). Urate is freely filtered by the glomerulus and essentially reabsorbed, because only 10% of the filtered load is present in the final urine (4). The transport mechanisms of urate are localized in the proximal tubule (PT), whereas no experimental evidence supports urate permeability in the more distal segments of the nephron (5). URAT1, the long-hypothesized apical urate-anion exchanger involved in the reabsorption of urate by PT cells, was recently identified (6). Inactivating mutations of URAT1 located on 11q13 are responsible

Received March 12, 2003. Accepted August 1, 2003.
Correspondence to Dr. Karin Dahan, Center for Human Genetics, Université Catholique de Louvain, Avenue E. Mounier 52, Tour Vésale 5220, B-1200, Brussels, Belgium. Phone: 0032-2-764-52-20; Fax: 0032-2-764-52-22; E-mail: Dahan@gmed.ucl.ac.be
KD and OD contributed equally to this study.
1046-6673/1411-2883
Journal of the American Society of Nephrology

DOI: 10.1097/01.ASN.0000092147.83480.B5

for idiopathic renal hypouricemia, a condition characterized by very low blood levels of urate as a result of increased urinary excretion of urate (6,7).

FJHN shares several characteristics with autosomal-dominant medullary cystic kidney disease (MCKD), a rare condition characterized by the development of chronic interstitial nephritis during adulthood, along with the (inconstant) detection of corticomedullary cysts (8–11). In fact, medullary cysts were found in several members of a Belgian family with FJHN (1), and a history of gout was reported in several families with MCKD (2,8–11). Two different loci for MCKD have been mapped, *MCKD1* on chromosome 1q21 (MCKD1) (12) and *MCKD2* on chromosome 16p12 (MCKD2) (13). Further mapping of FJHN on chromosome 16p11.2, at a very close location to *MCKD2*, raised the question as to whether distinct genes for MCKD2 and FJHN co-localize within the approximately 4.8-cM region or the two disorders represent phenotypic variants of a defect in a single gene (1,14,15). The latter hypothesis was recently confirmed by Hart *et al.* (16), who identified four mutations in the *UMOD* gene that encodes uromodulin/Tamm-Horsfall protein, as the cause of FJHN in three families and MCKD2 in one family. Five additional mutations in *UMOD* were last reported by Turner *et al.* (17) in five kindreds with FJHN. In this study, we report on the identification of 11 different mutations (10 of which are novel) in the highly conserved exon 4 of *UMOD* in 11 families with FJHN. We show that mutations in *UMOD* lead to an accumulation of uromodulin in cells lining the thick ascending limb (TAL) of Henle's loop, together with a drop in the urinary excretion of wild-type uromodulin. These observations could help to elucidate the role of uromodulin and better understand the renal tubular handling of urate.

Materials and Methods

Family Screening

Twenty-five families were investigated on the basis of a clinical picture strongly suggestive of FJHN disease, as defined by the following criteria: (*1*) a history of chronic renal failure (CRF) in at least two related family members with an inheritance compatible with an autosomal dominant trait; (*2*) exclusion of another well-defined hereditary nephropathy, especially Alport syndrome and hereditary focal segmental glomerulosclerosis; and (*3*) a history of gout or hyperuricemia (serum uric acid level >6 mg/dl) in all individuals with CRF. In each family, we defined as affected those with CRF and a history of gout/hyperuricemia as well as those with a serum creatinine ≤ 1.4 mg/dl and a serum concentration of uric acid higher than 1 SD of the normal values for age and gender (<5 yr, 3.6 ± 0.9; 5 to 10 yr, 4.1 ± 1; male >10 to 12 yr, 4.4 ± 1.1; male >12 to 18 yr, 5.6 ± 1.1; male >18 yr, 6.2 ± 0.8; female >10 to 12 yr, 4.5 ± 0.9; female >12 to 18 yr, 4.5 ± 0.9; female >18 yr, 4 ± 0.7 mg/dl (18)). CRF was graded according to the National Health and Nutrition Examination Survey III criteria: stage 1 (normal), GFR ≥ 90 ml/min; stage 2 (mild), 60 to 89 ml/min; stage 3 (moderate), 30 to 59 ml/min; stage 4 (severe), 15 to 29 ml/min (19).

Eight families were first analyzed by linkage to the critical region of *MCKD1* and *FJHN/MCKD2* on 1q21 (12) and on 16p12, respectively (1,13–15). Haplotype analysis excluded linkage to *MCKD1* locus in the eight tested families, whereas the markers selected from *FJHN/MCKD2* locus on 16p12 showed compatibility with a possible linkage to this chromosomal region in four of them. After the detection of mutations in the *UMOD* gene in the four families potentially linked to 16p12, we sequenced this gene in all available patients who belonged to the 21 other kindreds who met inclusion criteria.

Mutational Analysis

Mutational analysis of the uromodulin gene (*UMOD*) was performed using specific primers for the 5'- and 3'-flanking intron sequences. PCR primers were generated by alignment of genomic DNA to human and mouse mRNA and EST (Evidence View, November 2002, www.ncbi.nlm.nih.gov). We used 40 cycles of amplification using AmpliTaq Gold (Perkin Elmer Applied Biosystems) according the manufacturer's instructions. The amplicons generated were purified using a QIAquick PCR purification kit (Qiagen) and directly sequenced with the BigDye terminator kit (Perkin Elmer Applied Biosystems). Sequences were analyzed on an ABI3100 capillary sequencer (Perkin Elmer Applied Biosystems).

Intrarenal Expression and Urinary Excretion of Uromodulin

Human Kidney Samples. The immunostaining for uromodulin was tested on kidney samples from three FJHN patients with a defined *UMOD* mutations (F1-IV-11, F1-IV-12, F2-III-3). The two samples from the F1 family were end-stage kidneys removed during renal transplantation, whereas the F2 sample originated from a renal biopsy (serum creatinine, 3.2 mg/dl). Controls included two normal human kidney samples obtained at surgery; two samples from related patients with nephronophthisis as a result of a mutation in *NPHP1* and one sample from a patient with FJHN and no detected mutation in *UMOD*. These samples were routinely fixed in 4% formaldehyde and embedded in paraffin (20). The use of these samples has been approved by the University of Louvain Ethical Review Board.

Antibodies. A polyclonal sheep antibody (Biodesign International, Saco, ME) and a monoclonal mouse antibody (Cedarlane, Ontario, Canada) against human uromodulin were used (20,21). Other antibodies included a rabbit polyclonal antibody against human aquaporin-1 (AQP1; Chemicon, Temecula, CA), a rabbit polyclonal antibody against the human serotonin receptor 1A (SR1A; Santa Cruz Biotechnology, Santa Cruz, CA) (22), and a rabbit polyclonal antibody against human aquaporin-2 (AQP2; Alamone, Jerusalem, Israel).

Immunoblot Analyses and Deglycosylation Studies. Membrane extracts were prepared as described previously (20). Fresh morning urine samples were also obtained in six FJHN patients with a defined *UMOD* mutation and various degrees of renal failure (F3-III-1, F3-III-2, F4-IV-1, F6-II-1, F7-II-1, F7-II-2), one patient with renal failure as a result of FJHN without *UMOD* mutation, six control patients with renal failure related to another nephropathy (reflux nephropathy, $n = 2$; autosomal dominant polycystic kidney disease, $n = 2$; chronic glomerulonephritis, $n = 2$), and two normal subjects. In some experiments, urine samples in the Laemmli buffer were prepared in reduced (100 mM DTT, followed by 5 min heating at 95°C) or nonreduced conditions. For deglycosylation experiments, 10 μl of urine was incubated for 6 h at 37°C with 12 units of N-glycosidase F (Roche, Vilvoorde, Belgium).

The samples were separated by SDS-PAGE and transferred to nitrocellulose (20). After blocking, membranes were incubated overnight at 4°C with primary antibodies, washed, incubated for 1 h at room temperature with appropriate peroxidase-labeled antibodies (Dako, Glostrup, Denmark), washed again, and visualized with enhanced chemiluminescence. Specificity of the immunoblot was deter-

mined by co-migration with purified human uromodulin (Biomedical Technologies, Stoughton, MA) and incubation with nonimmune IgG (Vector Laboratories, Burlingame, CA). Densitometry analysis was performed with a Hewlett Packard Scanjet model (4-channel video capture card)IVC using the NIH Image V1.60 software, and optical densities were normalized to the normal control sample density. The immunoblots were performed in triplicate.

Immunoprecipitation and Mass Spectrometry. Urine samples (1 ml) of control subjects and patients with *UMOD* mutations (F3-III-1, F4-IV-1) were incubated with monoclonal or polyclonal anti-uromodulin antibodies for 3 h at 4°C. After centrifugation (12,000 × *g* for 5 min), protein G-Sepharose (Zymed Laboratories, San Francisco, CA) was added to the supernatant and incubated overnight at 4°C. The immune complexes were washed and boiled in Laemmli buffer containing DTT, before migration in 7.5% SDS-PAGE. After staining with Coomassie Bio-Safe (Bio-Rad, Hercules, CA), the protein bands were digested and analyzed by mass spectrometry as described (23).

Immunostaining. Six-micrometer sections were cut from paraffin blocks, rehydrated, and incubated for 30 min with 0.3% hydrogen peroxide to block endogenous peroxidase. After incubation with 10% normal serum in PBS for 20 min, sections were incubated for 45 min with the primary antibodies diluted in PBS containing 2% BSA. After three washes of 5 min each, sections were incubated with the appropriate biotinylated secondary anti-IgG antibody (Vector Laboratories), washed again, and incubated for 45 min with the avidin-biotin peroxidase complex (Vectastain Elite; Vector Laboratories). Before visualization with aminoethylcarbazole (Vector Laboratories), sections were viewed under a Leica DMR-DC300 photomicrographic system (Leica, Heerbrugg, Switzerland). The specificity of immunostaining was tested by incubation (*1*) in absence of primary antiserum and (*2*) with nonimmune rabbit serum or control rabbit or mouse IgG (Vector Laboratories).

Results

Sequencing Analysis

Mutational analysis of *UMOD* gene was performed in affected individuals from 25 families by direct sequencing of forward and reverse strands of exon-PCR products. Eleven heterozygous mutations of which 10 are novel were detected in the fourth coding exon of *UMOD* in all individuals considered to be affected among 11 families (Table 1). No disease-specific

Table 1. Clinical characteristics, histological findings, and type of mutation in the *UMOD* gene among 11 families with FJHN[a]

Family	Origin	No. of individuals with *UMOD* mutation	Clinical phenotype			Cysts[c]	Renal histology	Mutation	
			Renal function	Age[b]	Gout/age at first attack			Nucleotide change	Effect on coding sequence
F1	Belgium	6	ESRF	28, 36, 40, 42, 54, 63	+ (6/6)/8, 18, 19, 26, 32, ND	+ (3/3)	3/3 TIN	C658A	Arginine → Serine R185S
		5	NL	7, 10, 16, 22, 34	− (5/5)	ND	ND		
F2	France (Corsica)	1	ESRF	47	+/34	− (1/1)	ND	G770C	Arginine → Proline R222P
		6	CRF	23, 26, 38, 44, 45, 54	+ (3/6)/21, 23, 28	+ (2/2)	2/2 TIN		
F3	France	1	ESRF	38	+/14	ND	ND	668del99	In-frame deletion
		2	CRF	9, 12	− (2/2)	ND	ND		
F4	France	2	CRF	72, 73	− (2/2)	+ (1/2)	ND	G614A	Cysteine → Thyrosine C170Y
		1	NL	33	−	ND	ND		
F5	Italy	1	ESRF	52	+/31	ND	ND	T481C	Cysteine → Arginine C126R[d]
		1	CRF	31	+/20	ND	ND		
F6	Belgium	1	ESRF	64	+/30	+	ND	T439C	Cysteine → Arginine C112R
F7	Morocco	1	CRF	57	+/38	−	ND	C715G	Arginine → Glycine R204G
F8	Belgium	1	ESRF	59	−	+	ND	A281C	Aspartate → Alanine D59A
F9	France	4	ESRF	38, 52, 58, 60	+ (1/4)/15	+ (1/1)	1/4 TIN	C779T	Threonine → Methionine T225M
		3	CRF	34, 35, 40	− (3/3)	ND	ND		
		1	NL	34	−	ND	ND		
F10	France	1	ESRF	25	+/14	ND	ND	T949C	Cysteine → Arginine C282R
F11	Belgium	1	ESRF	36	+/21	−	ND	T794G	Cysteine → Glycine C217G

[a] ESRF, end stage renal failure; CRF, chronic renal failure; NL, normal renal function; TIN, tubulointerstitial nephritis; ND, no data available.
[b] Age at the time of examination or at ESRF.
[c] Detected by renal imaging (ultrasonography or CT).
[d] Mutation previously reported (22).

mutations were detected elsewhere in the *UMOD* gene (Figure 1).

Five mutations were a missense mutation involving a cysteine residue: Cys112Arg (C112R), Cys126Arg (C126R), Cys170Tyr (C170Y), Cys217Gly (C217G), and Cys282Arg (C282R). The substitution involving the cysteine at position 126 was previously reported by Turner *et al.* (17) in another family with FJHN. The replacement of cysteine residue is predicted to cause misfolding by removal of a disulfide bond that stabilizes the native domain fold.

Five other mutations resulted in the replacement of another residue: Asp59Ala (D59A), Arg185Ser (R185S), Arg204Gly (R204G), Arg222Pro (R222P), and Thr225Met (T225M). All resulted in the substitution of structurally conserved residue in *UMOD* homologues from different species and belonging to different polarity groups. The mutation observed in family F2 resulted in an arginine-to-proline amino acid change for a residue only conserved in mouse and rat at position 222 in the protein (R222P). In bovine uromodulin, the amino acid position equivalent to R222 is occupied by another dibasic amino acid, histidine. This clearly suggests that the basic polarity may be functionally significant and that the substitution to the neutral amino acid probably affects their structure and function.

The last mutation was an in-frame deletion between nucleotides 668 and 767 (668del99). This deletion is predicted to cause a replacement of conservative Glu188 by an irrelevant valine and to remove 33 amino acids including two of 24 consecutive cysteine residues following the Glu188.

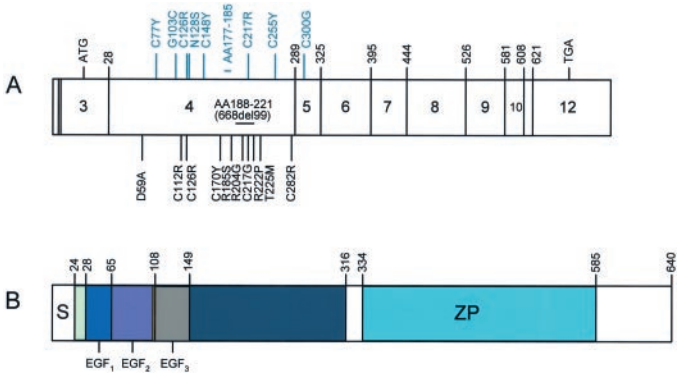

Figure 1. Schematic representation of *UMOD* gene showing genomic structure, known protein domains, and mutations observed in 20 unrelated patients. (A) Exon structure of *UMOD* transcript with locations of *UMOD* mutations. Boxes represent the 12 exons encoding uromodulin. The number of the first codon of each exon is indicated. The GenBank *UMOD* mRNA (accession no. NM_024915) is 2290 nucleotides with an open reading frame predicted to encode uromodulin, a 640–amino acid protein (24–26). The start codon begins at nucleotide 106 corresponding to the third exon. The nine different mutations previously reported by Hart *et al.* (16) and Turner *et al.* (17) and the 11 mutations (10 of which are novel) identified in this study are shown above (light blue) and below (black) the transcript, respectively; missense mutations and deletions are represented by vertical and horizontal bars, respectively. (B) *UMOD* predicted protein structure: functional domains of *UMOD* are shown as shaded boxes, with their names. The N-terminal region (essentially exon 4) contains three epidermal growth factor (EGF)-like modules with typical Ca^{2+}-binding consensus in two of them (cbEGF2 and cbEGF3) followed by a cysteine-rich sequence of 166 residues that are highly conserved in *UMOD* homologues from different species (24). The C-terminal region contains the zona pellucida (ZP), an approximately 260–amino acid domain that is responsible for polymerization of this protein into filaments of similar supramolecular structure (26) and a phosphatidylinositol anchor (between codons Leu^{601} and Ala^{616}) (25).

Clinical Findings

The main clinical characteristics available in the 39 patients from 11 families with an identified mutation in *UMOD* are summarized in Figure 2 and Table 1. At the time of examination, seven individuals had a preserved renal function, 15 had CRF, and 17 had reached ESRF between the age of 25 and 64. Of note, autonomous renal function was maintained in two affected individuals in their eighth decade (F4-III-2, F4-III-3). A history of gout was recorded in 18 individuals from nine kindreds with an onset ranging from 8 to 38 yr. Kidney tissue specimens, available in six subjects belonging to F1, F2, and F9, revealed in each case a picture of chronic interstitial nephritis with tubular atrophy and a marked thickening of tubular basement membranes, as previously reported (1,2). A renal imaging study, available in 12 patients from eight families, all with CRF or ESRF, revealed the presence of cysts (most often of small size, within uniformly shrunken parenchyma) in nine of them. The mutation was absent in 16 of 16 unaffected individuals.

Effect of UMOD Mutations on Urinary Excretion and Renal Expression of Uromodulin

Expression of Uromodulin in the Kidney and Urine: Immunoblot Analyses. The polyclonal antibody against human uromodulin detected a single band at the expected size of approximately 85 to 90 kD (27,28) in normal human kidney and urine samples (Figure 3A). A faster migration of the immunoreactive band was observed in nonreduced *versus* reduced urine samples. These bands co-migrated with purified human uromodulin, and no signal was detected when identical blots were probed with nonimmune IgG. Similar results were obtained with the monoclonal antibody, which showed a very strong affinity for uromodulin in the urine (data not shown). The nature of uromodulin excreted in the urine was investigated by immunoblotting analyses in reduced, nonreduced, and deglycosylated conditions, using samples from two affected members of the F3 family with an in-frame deletion in *UMOD* *versus* three patients with missense mutations and two normal controls. As shown in Figure 3B, the migration pattern of urinary uromodulin in reduced, nonreduced, and deglycosylated conditions did not differ between patients and control subjects. Assuming that loss of cysteine residues or truncation would modify the migration pattern of mutated uromodulin, these data support the hypothesis that only wild-type uromodulin is excreted in the urine of patients with FJHN with *UMOD* mutation. This hypothesis was confirmed by the analysis of uromodulin purified from the urine of control subjects and

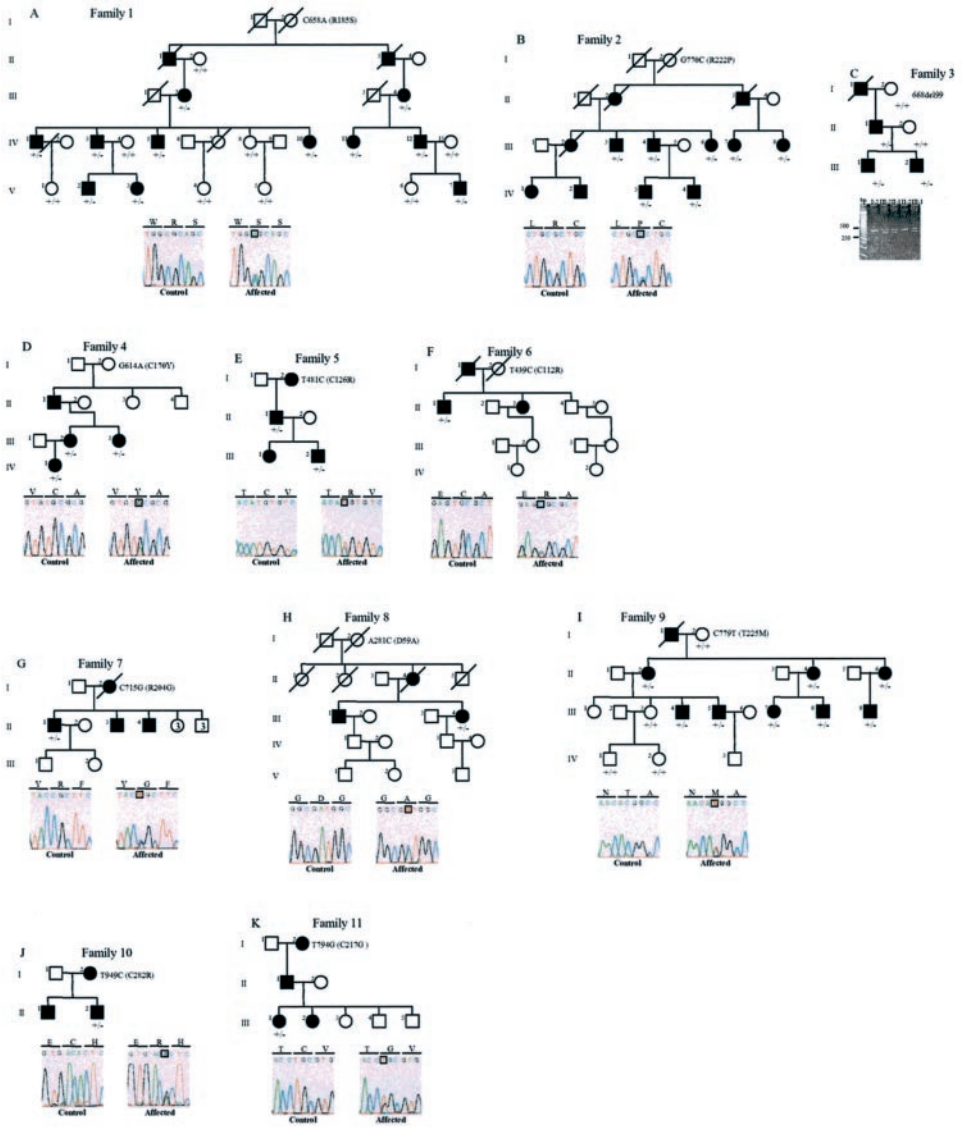

Figure 2. UMOD gene mutations in 11 families with familial juvenile hyperuricemic nephropathy (FJHN)/medullary cystic kidney disease (MCKD2) disease. For each kindred with *UMOD* mutation, the genealogical tree is shown, as well as two electropherograms, corresponding to a patient and a control DNA (except for family F3). Migration of the PCR products from family F3 shows abnormal bands for the three affected relatives corresponding to a 99-bp deletion in exon 4, confirmed by direct sequencing (data not shown). The upper band is the normal allele of 483 bp; the lower is the mutant allele of 384 bp. Carriers and noncarriers of *UMOD* mutation are represented by 178 +/− 178 and 178 +/+ 178, respectively; all other individuals are untested for mutation.

FJHN patients with *UMOD* mutations. Immunoprecipitation with both anti-uromodulin antibodies yielded a single band at 85 to 90 kD in urine samples from patients and control subjects. The band co-migrated with purified uromodulin, and analysis by mass spectrometry confirmed that it corresponded to wild-type uromodulin (data not shown).

The band corresponding to uromodulin was detected with variable intensity in urine samples obtained from normal control subjects, patients with *UMOD* mutations, and patients with renal failure attributed to other causes (Figure 3C). The samples were divided in three categories according to the degree of renal failure and normalized for urinary creatinine excretion. In comparison with normal control subjects, the urinary excretion of uromodulin was decreased in patients with renal failure. Furthermore, within each category, patients with *UMOD* mutations had a systematically lower uromodulin excretion than other patients with a similar degree of renal failure. It must be noted that the decrease in uromodulin excretion seems to be specifically related to *UMOD* mutations because it was not observed in patients with renal failure as a result of FJHN without mutation in this gene (Figure 3D).

Distribution of Uromodulin and Tubular Markers in the Kidney: Immunohistochemistry. The segmental distribution and staining pattern of uromodulin was investigated in kidneys with proven *UMOD* mutations *versus* normal kidneys and kidneys from patients with interstitial nephropathies sim-

ilar to FHJN but without *UMOD* mutation (Figure 4). In the normal human kidney (Figure 4, A to G), uromodulin is distributed primarily in the TAL and distal convoluted tubule (DCT) segments (Figure 4A), with a staining pattern characteristic of apical membrane reactivity (Figure 4B). The segmental distribution to the TAL in the medulla was ascertained by lack of cross-reactivity with AQP1 (a marker of descending thin limbs; Figure 4, C and D) and AQP2 (a marker of the collecting ducts, data not shown) and co-distribution with SR1A on serial sections (Figure 4, E and F) (22). It must be noted that the discrete apical staining pattern was observed with both antibodies and that no specific staining was detected when incubation was performed with non-immune IgG (Figure 4G).

Significant modifications in the expression and staining pattern for uromodulin were detected in the three kidneys from patients with a *UMOD* mutation (Figure 4, H to O). Intense staining for uromodulin was detected in a limited number of tubule profiles that sometimes were enlarged or even cystic (Figure 4, H and I). Staining on serial sections demonstrated that tubule profiles positive for uromodulin were not stained for AQP1, thus excluding proximal tubule reactivity (Figure 4, I and J). At higher magnification, the intense staining for uromodulin was diffusely intracellular, with intratubular heterogeneity. The staining pattern was similar in the three FJHN kidneys (Figure 4, K to M). Staining on serial sections showed that tubule profiles with abnormal expression of uromodulin were positive for SR1A, confirming the segmental distribution in TAL (Figure 4, N and O). The abnormal staining pattern and intensity for uromodulin was specific to patients with *UMOD* mutations, because it was not observed in kidneys from patients with nephronophthisis and FJHN without *UMOD* mutation (Figure 4, P and Q). Similar observations were made with both monoclonal and polyclonal antibodies against uromodulin.

Discussion

We have identified 10 novel mutations in the *UMOD* gene in 11 families with FJHN. These data extend two previous studies in which nine mutations in *UMOD* were detected in eight families with FJHN and one with MCKD2 (16,17). The clinical profile of the affected subjects from these 20 families is similar, with hyperuricemia and/or gout as an early manifestation and the later development of chronic interstitial nephritis. The detection of medullary cysts in nine of 12 individuals belonging to eight families with FJHN (F1, F2, F4, F6, to F9, and F11; Table 1) confirms our earlier observations (1). Both clinical and genetic findings therefore support our suggestion that FJHN and MCKD2 represent two facets of the same entity (1).

The *UMOD* gene thus is responsible for a significant subset of cases of FJHN/MCKD, as evidenced by mutation detection in 44% of the families with this condition. Another gene responsible for MCKD has been mapped on chromosome 1q21 (12,29,30). Although the clinical picture was indistinguishable from FJHN in one of these seven families (10), there was no history of gout or hyperuricemia in the six others (29,30). Because we have excluded linkage to both *MCKD1* and

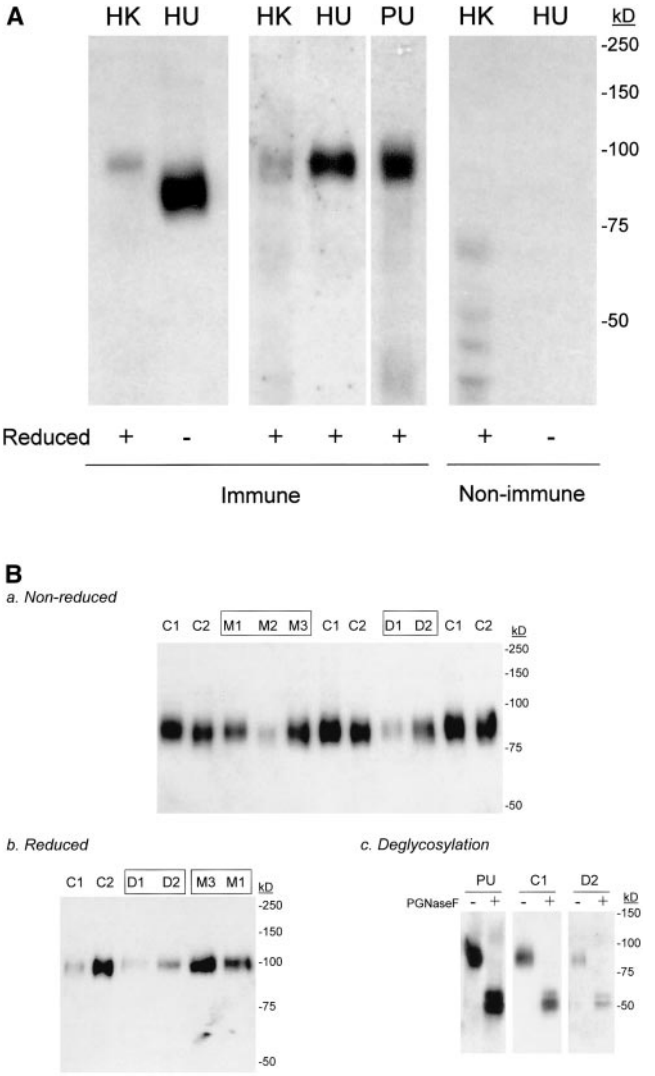

Figure 3. Detection of uromodulin in the human kidney and urine: immunoblotting. (A) Normal human kidney (HK; 20 μg) and urine (HU; 4 μl) and purified uromodulin (PU; 0.5 μg) were subjected to 7.5% SDS-PAGE, transferred to nitrocellulose, and probed with polyclonal sheep antibodies against uromodulin (immune lanes) or nonimmune IgG at the same dilution (nonimmune lanes). The broad band at approximately 85 to 90 kD in the HK and HU corresponds to the predicted size of uromodulin and co-migrates with purified uromodulin. Note that uromodulin migrates faster in nonreduced than in reduced samples. No specific signal was detected on blots probed with nonimmune IgG. (B) Qualitative analysis of uromodulin migration in nonreduced *versus* reduced urine samples and after deglycosylation. Urine samples from normal control subjects (C1 and C2, 1 to 1.5 μl), FJHN patients with three different missense mutations of *UMOD* (M1 to M3, 5 to 15 μl), and two FJHN patients from the F3 family with a deletion of *UMOD* (D1 and D2, 10 to 15 μl) were probed in reducing or nonreducing conditions with anti-uromodulin polyclonal antibodies. The migration pattern of uromodulin in both conditions is similar in control subjects and patients with *UMOD* mutations. PU as well as urine samples from a normal control subject (C1) and an FJHN patient with a deletion in *UMOD* (D2) were incubated with (+) or without (−) N-glycosidase F, separated on 7.5% PAGE, and probed with polyclonal anti-uromodulin antibodies. The shift of the uromodulin band to a lower apparent molecular weight confirms the existence of Asn-linked glycan chains. Note that the deglycosylated pattern (duplicate band) is exactly similar for the three samples.

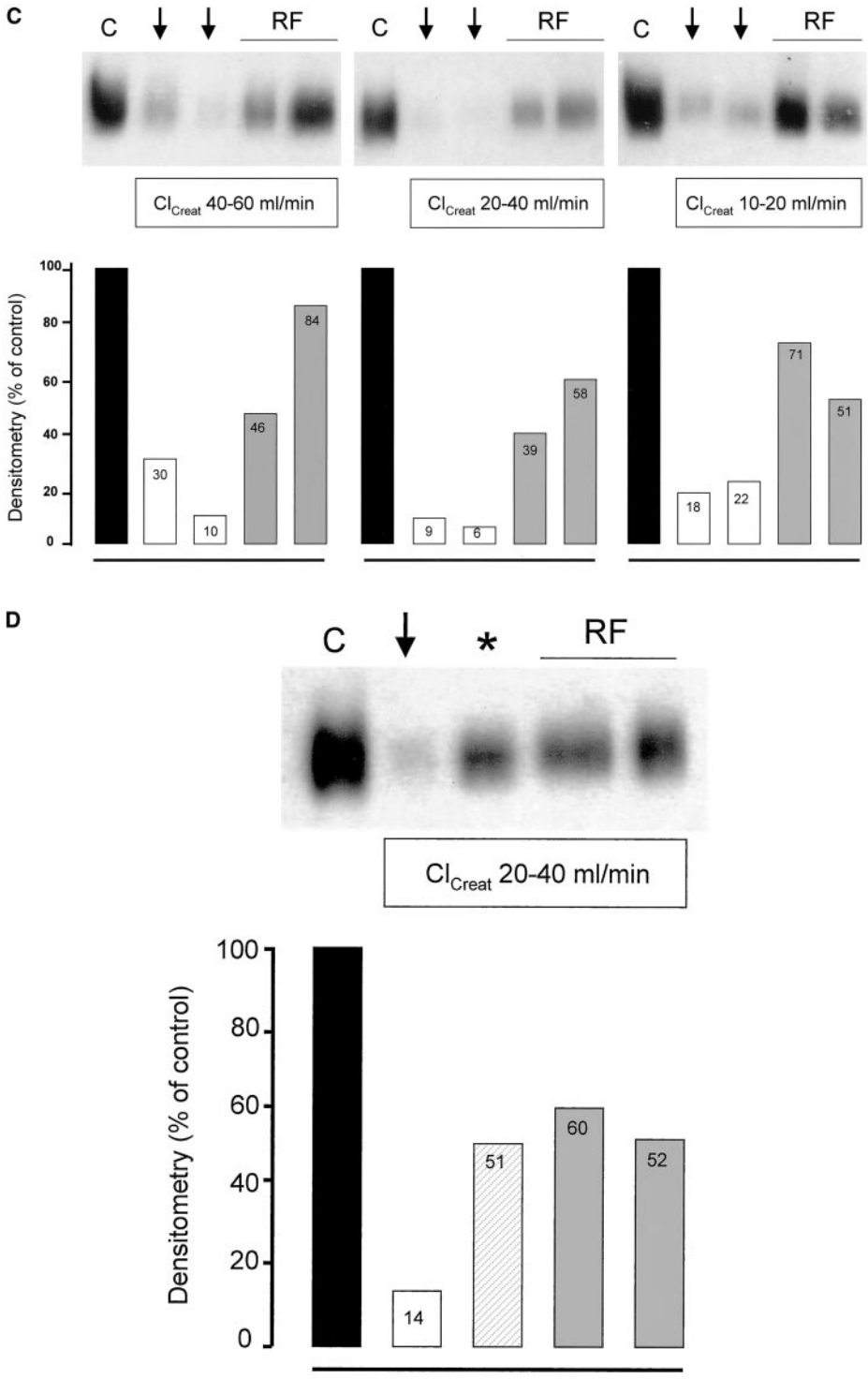

Figure 3. (C) Quantitative analysis of uromodulin excretion in the urine. Detection of uromodulin in urine samples obtained from a normal control subject (C), six patients with *UMOD* mutations (arrows), and six patients with renal failure attributed to other causes (RF; top). The patients were divided in three categories according to the degree of renal failure (see creatinine clearance values boxed), and the amount of urine loaded within each subgroup was normalized for urinary creatinine. The urinary excretion of uromodulin is decreased in all patients with renal failure as compared with normal control subjects. Within each category, patients with *UMOD* mutations (F4-IV-1 and F3-III-2, F7-II-1 and F3-III-1, F6-II-1 and F6-II-2) show a systematically lower uromodulin excretion than non-FJHN patients with a similar degree of renal failure. These observations are confirmed by densitometry analysis (bottom). (D) Specificity of the decreased urinary excretion of uromodulin. Urine samples from a normal control subject (C), two FJHN patients with either a missense mutation of *UMOD* (arrow) or without *UMOD* mutation detected (asterisk), and two patients with renal failure unrelated to FJHN (RF) were probed with polyclonal antibodies against uromodulin. The urinary excretion of uromodulin is significantly lower in the FJHN patient harboring an *UMOD* mutation *versus* other patients with renal failure. The loading was normalized for urinary creatinine.

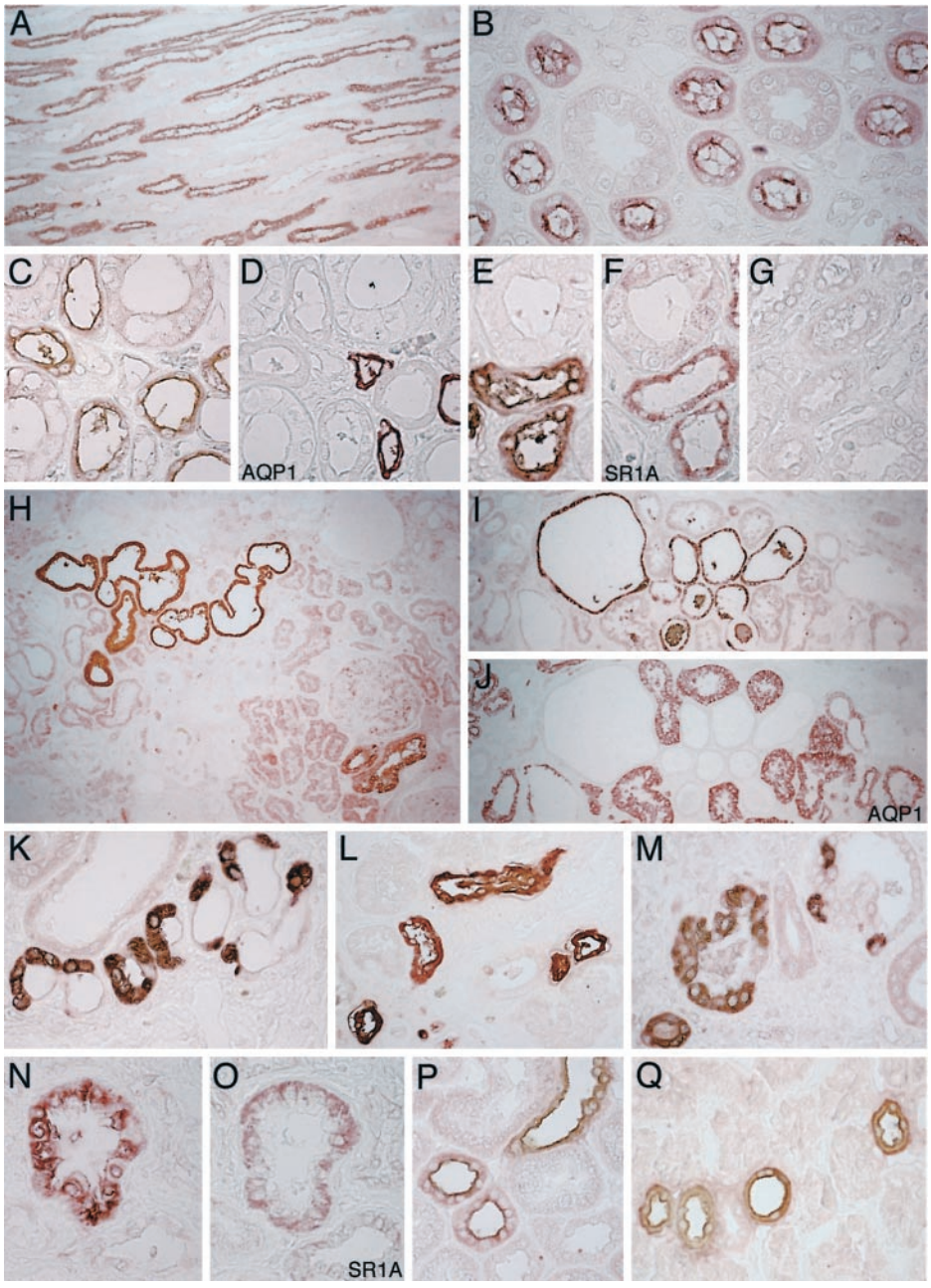

Figure 4. Expression patterns and distribution of uromodulin in the kidney: immunohistochemistry. The segmental distribution and staining pattern of uromodulin was compared in normal kidneys (A to G), three kidneys with proven *UMOD* mutations (H to O), and kidneys from patients with nephronophthisis (P) and FHJN without *UMOD* mutations (Q). In the normal human kidney, uromodulin is distributed primarily in the thick ascending limb (TAL) segments (A), with a distinct apical membrane reactivity (B). The segmental distribution to the TAL was demonstrated by lack of cross-reactivity with aquaporin 1 (AQP1; C and D) and AQP2 (not shown) and co-distribution with SR1A on serial sections (E and F). No specific staining was detected when using nonimmune IgG (G). Polyclonal sheep antibodies against uromodulin were used in A, C, and E (1:200); and monoclonal antibody was used in B (1:100). The expression and staining pattern for uromodulin was significantly modified in the three kidneys harboring *UMOD* mutations (F1-IV-11 [H and M], F1-IV-12 [I to K and N and O], and F2-III-3 [L]). Intense staining for uromodulin was detected in a subset of tubule profiles (H and I) that are sometimes enlarged or cystic. The tubule profiles stained for uromodulin are negative for AQP1 (I and J). At higher magnification, the staining for uromodulin is intense, diffusely intracellular, and also heterogeneous within tubular cells (K to M). The tubule profiles with abnormal expression of uromodulin were positive for SR1A, confirming the segmental distribution in TAL (N and O). The abnormal staining pattern and intensity for uromodulin is not observed in patients with other types of interstitial nephropathies, such as nephronophthisis (P) and FJHN unrelated to *UMOD* mutation (Q). Polyclonal sheep antibodies against uromodulin were used in H, K to N, P, and Q (1:200); and monoclonal antibody in I (1:100). Magnification: ×80 in A, H, I, and J; ×320 in B to G and K to Q.

MCKD2 in four of eight families, the existence of at least a third locus for FJHN is confirmed (15,29,31). It is interesting that a mutation in the HNF-1β gene was recently identified in a family with FJHN (32).

The *UMOD* gene encodes uromodulin, a 85-kd glycoprotein that is identical to the Tamm-Horsfall protein (24,25). Although uromodulin is the most abundant protein in the normal urine (33), its biologic role remains enigmatic. Uromodulin is a glycosylphosphatidylinositol (GPI) anchor-linked protein that is located to the apical membrane of tubular cells lining the TAL and DCT (34). The roles of uromodulin in the kidney may include modulation of cell adhesion (35) and signal transduction by interaction with protein kinases (36) and, more specific, inhibition of calcium oxalate crystal aggregation, formation of urinary casts, defense against urinary tract infection, and modulation of urine concentrating ability (28). Uromodulin has also been regarded as a potential nephritogenic antigen (37).

The 10 novel mutations of *UMOD* (nine missense and one in-frame deletion), like eight others reported previously (16,17), are located between codons 59 and 282 of exon 4, providing strong evidence of a hot spot region within the 5' coding region of the gene. Only one disease-specific mutation has been detected elsewhere in the *UMOD* gene, the Cys300Gly substitution identified in exon 5 (17) (Figure 1A). The mechanism(s) by which these exon-specific mutations in *UMOD* cause disease remain(s) to be elucidated. It is interesting that no mutation is predicted to result in premature termination of translation. The clustering of mutations in exon 4 is likely to be significant considering (*1*) a strong sequence conservation in evolution (38); (*2*) an approximately 53% sequence similarity with glycoprotein-2 (GP-2), a zymogen granule GPI-linked protein that, like uromodulin, is released from apical membranes to form large aggregates in solution (34,39); (*3*) the high number of cysteine residues in this part of the protein (24); and (*4*) the presence of three epidermal growth factor-like (EGF) repeats, able to interact with structurally related ligands (24,25,40) (Figure 1B). EGF domains represent one of the most commonly identified protein modules that mediate protein–protein interactions (40). A subset of these domains contains a calcium-binding (cb) consensus sequence (40). This type of EGF domain has been identified in many proteins, including the human fibrillin and Notch family proteins (41,42). Furthermore, genetic mutations that cause amino acid changes within cbEGF in these proteins have been linked to human diseases, including the Marfan syndrome (41) and cerebral autosomal-dominant arteriopathy with subcortical infarcts and leukoencephalopathy (42). It is interesting that six missense mutations that have been associated with FJHN occur within cbEGF2 and cbEGF 3 (Figure 1). These mutations can be classified into two groups depending on the residue affected. Mutations that affect cysteine residues are likely to alter disulfide bond formation, thereby disrupting the correct protein folding (43), and mutations that affect residues in the cb consensus sequence are likely to reduce cb affinity, leading to structural destabilization, as suggested by Turner *et al.* (17) for the substitution N128S.

Our study of uromodulin expression in the urine and kidney biopsies of nine patients with *UMOD* mutations (four families) provides interesting information on the consequences of these mutations. Immunoblotting studies (Figure 3) demonstrated a consistent decrease in the urinary excretion of uromodulin in patients with *UMOD* mutations, by comparison with normal control subjects and patients with renal failure as a result of other causes, including FJHN without *UMOD* mutation. The migration pattern in reduced, nonreduced, and deglycosylated samples, as well as analyses by mass spectrometry, confirmed that the immunoreactive protein excreted in the urine was the wild-type uromodulin. In the normal kidney, uromodulin expression is restricted to the TAL and DCT (44) (Figure 4). In three patients, all carriers of a missense mutation, we documented a marked increase in the expression of uromodulin in a subset of tubule profiles, that sometimes appeared dilated, distorted, or cystic (Figure 4). These tubule profiles did not include PT but had the characteristics of the TAL (positive for SR1A and negative for AQP1). In positive tubules, the staining pattern for uromodulin was diffusely intracellular, with some heterogeneity among tubular cells. This pattern of uromodulin expression seems to be specific of *UMOD* mutations, because it was not found in two related cases of juvenile nephronophthisis and one case of FJHN without *UMOD* mutation. Taken together, our data suggest that only wild-type uromodulin is excreted in the urine of patients with *UMOD* mutations, whereas mutated uromodulin accumulates within tubular cells. The accumulation could result from (*1*) a gain of function leading to an increased production of uromodulin, (*2*) an abnormal targeting (by disturbance of the GPI anchor signal) (45), or (*3*) an impaired clearance of the protein from the epithelial cell surface through a gain of resistance to proteolytic cleavage (46).

Our findings support previous observations (47,48) indicating that hyperuricemia is the primary clinical finding in FJHN. Hyperuricemia was indeed present in five individuals $\leq$16 yr old from F1 and F3 families who were carriers of mutation (Table 1). However, Hart *et al.* (16) reported that four women who carried a *UMOD* mutation had a normal serum uric acid level (despite a low fractional excretion of uric acid). Conversely, we found hyperuricemia in one obese woman from F1 who lacked the mutation. This emphasizes the value of mutation analysis for an accurate early diagnosis of carrier of the disease.

It was unexpected that mutations in *UMOD* are responsible for a disease characterized primarily by hyperuricemia and low urinary excretion of urate. The tubular reabsorption of urate in the human nephron is confined to the PT (4), where it is thought to be mediated by URAT1 (6). The basolateral pathway of urate is less characterized and may involve multispecific organic anion transporter proteins (6). Much less is known about the secretion and postsecretory reabsorption of urate in the PT or more distal nephron segments (4). Our data clearly show that the abnormal expression of uromodulin in kidneys with *UMOD* mutations does not involve PT cells, which argues against a direct role of abnormal uromodulin in urate reabsorption by PT cells. Uromodulin might also affect urate transport through an effect on NaCl reabsorption in the TAL (44,49).

Accordingly, an abnormal expression of the mutated uromodulin in the TAL, such as evidenced by our studies, could decrease NaCl reabsorption and subsequently induce a state of volume contraction that is known to promote the proximal reabsorption of urate (50). Another unanswered question is whether early hyperuricemia plays a role in the development of chronic interstitial nephritis or, alternatively, is an independent manifestation of the disease. Conflicting results on the effect of allopurinol on disease progression have been reported (47,51). Mutagenesis of *UMOD* in the mouse could shed light on this issue, because in this species, uricase activity is preserved (4).

In summary, our study points to a mutation clustering within exon 4 of *UMOD* as the underlying genetic defect in a significant subset of FJHN. Sequencing of exon 4 of the *UMOD* gene becomes the first diagnostic test in patients with chronic interstitial nephritis of undetermined origin with a history of gout or hyperuricemia, even in the absence of family history of renal disease. Furthermore, mutations in *UMOD* lead to aberrant expression of the protein in tubular cells that could play a role in the development of hyperuricemia and chronic interstitial nephritis.

Acknowledgments

This work was supported by grants from the Fonds de la Recherche Scientifique Médicale (Conventions 3.4539.03 and 3.4552.02), the Communauté Française de Belgique, the Federal Program Interuniversity Poles of Attraction (P5/05, Belgium), the Directorate of General Higher Education and Scientific Research, the Fondation Alphonse et Jean Forton, and the Action de Recherches Concertées (00/05-260).

We express our gratitude to the members of the Belgian family, to Drs. J.-P. Charmes, J.-F. De Plaen, J.-J. Lafontaine, H. Nivet, J.-M. Pochet, and B. Georges for referring patients; and to I. Abinet, Y. Cnoops, F. Jouret, and S. Nadalin for excellent assistance.

Electronic-Database Information

Accession numbers and URL for data in this article are as follows: Online Mendelian Inheritance in Man (OMIM), www.ncbi.nmn.nih.gov/omim (for FJHN [MIM 162000], MCKD1 [MIM 174000], MCKD2 [MIM 603860], MFS [154700], CADASIL [MIM 125310], NPH1 [MIM 256100], HYPOURICEMIA RENAL [MIM 220150]). Locus Link, www.ncbi.nlm.nih.gov:80/LocusLink/.

References

1. Dahan K, Fuschshuber A, Adamis S, Smaers M, Kroiss S, Loute G, Cosyns JP, Hildebrandt F, Verellen-Dumoulin C, Pirson Y: Familial juvenile hyperuricemic nephropathy and autosomal dominant medullary cystic kidney disease type 2: Two facets of the same disease? *J Am Soc Nephrol* 12: 2348–2357, 2001
2. Pirson Y, Loute G, Cosyns JP, Dahan K, Verellen C: Autosomal-dominant chronic interstitial nephritis with early hyperuricemia. *Adv Nephrol Necker Hosp* 30: 357–369, 2000
3. Oda M, Satta Y, Takenaka O, Takahata N: Loss of urate oxidase activity in hominoids and its evolutionary implications. *Mol Biol Evol* 19: 640–653, 2002
4. Roch-Ramel F, Guisan B: Renal transport of urate in humans. *News Physiol Sci* 14: 80–84, 1999
5. Burckhardt G, Pritchard JB: Organic anion and cation antiporters. In: *The Kidney, Physiology and Pathophysiology*, edited by Seldin DW, Giebisch G, Philadelphia, Lippincott Williams & Wilkins, 2000, pp 193–222
6. Enomoto A, Kimura H, Chairoungdua A, Shigeta Y, Jutabha P, Cha S, Hosoyamada M, Takeda M, Sekine T, Igarashi T, Matsuo H, Kikuchi SH, Oda T, Ichida K, Hososya T, Shimokata K, Niwa T, Kanai Y, Endou H: Molecular identification of a renal urate anion exchanger that regulates blood urate levels. *Nature* 417: 447–452, 2002
7. Igarashi T, Sekine T, Sugimura H, Hayakawa H, Arayama T: Acute renal failure after exercise in a child with renal hypouricaemia. *Pediatr Nephrol* 7: 292–293, 1993
8. Thompson GR, Weiss JJ, Goldman RT, Rigg GA: Familial occurrence of hyperuricemia, gout, and medullary cystic disease. *Arch Intern Med* 138: 1614–1617, 1978
9. Burke JR, Inglis JA, Craswell PW, Mitchell KR, Emmerson BT: Juvenile nephronophthisis and medullary cystic disease—The same disease (report of a large family with medullary cystic disease associated with gout and epilepsy). *Clin Nephrol* 18: 1–8, 1982
10. Stavrou C, Pierides A, Zouvani I, Kyriacou K, Antignac C, Neophytou P, Christodoulou K, Deltas CC: Medullary cystic disease with hyperuricemia and gout in a large Cypriot family: No allelism with nephronophthisis type I. *Am J Med Genet* 77: 149–154, 1998
11. Scolari F, Ghiggeri GM, Casari G, Amoroso A, Puzzer D, Caridi GL, Valzorio B, Tardanico R, Vizzardi V, Savoldi S, Viola BF, Bossini N, Prati E, Gusmano R, Maiorca R: Autosomal dominant medullary cystic disease: A disorder with variable clinical pictures and exclusion of linkage with the NPH1 locus. *Nephrol Dial Transplant* 13: 2536–2546, 1998
12. Christodoulou K, Tsingis M, Stravou C, Eleftheriou A, Papapavlou P, Patsalis PHC, Ioannou P, Pierides A, Constantinou, Deltas C: Chromosome 1 localization of a gene for autosomal dominant medullary cystic kidney disease (ADMCKD). *Hum Mol Genet* 7: 905–911, 1998
13. Scolari F, Puzzer D, Amoroso A, Caridi G, Ghiggeri GM, Maiorca R, Aridon P, De Fusco M, Ballabio A, Casari G: Identification of a new locus for medullary cystic disease, on chromosome 16p12. *Am J Hum Genet* 64: 1655–1660, 1999
14. Kamatani N, Moritani M, Yamanaka H, Takeuchi F, Hosoya T, Itakura M: Localization of a gene for familial juvenile hyperuricemic nephropathy causing underexcretion-type gout to 16p12 by genome-wide linkage analysis of a large family. *Arthritis Rheum* 43: 925–929, 2000
15. Stiburkova B, Majewski J, Sebesta I, Zhang W, Ott J, Kmoch S: Familial juvenile hyperuricemic nephropathy: Localization of the gene on chromosome 16p11.2—And evidence for genetic heterogeneity. *Am J Hum Genet* 66: 1989–1994, 2000
16. Hart TC, Gorry MC, Hart PS, Woodard AS, Shihabi Z, Sandhu J, Shirts B, Xu L, Zhu H, Barmada MM, Bleyer AJ: Mutations of the UMOD gene are responsible for medullary cystic kidney disease 2 and familial juvenile hyperuricaemic nephropathy. *J Med Genet* 39: 882–892, 2002
17. Turner JJ, Stacey JM, Harding B, Kotanko P, Lhotta K, Puig JG, Roberts I, Torres RJ, Thakker RV: UROMODULIN mutations cause familial juvenile hyperuricemic nephropathy. *J Clin Endocrinol Metab* 88: 1398–401, 2003
18. Wilcox WD: Abnormal serum uric acid levels in children. *J Pediatr* 128: 731–737, 1996
19. Garg AX, Kiberd BA, Clark WF, Haynes RB, Clase CM: Albuminuria and renal insufficiency prevalence guides population

screening: Results from the NHANES III. *Kidney Int* 61: 2165–2175, 2002
20. Devuyst O, Christie PT, Courtoy PJ, Beauwens R, Thakker RV: Intra-renal and subcellular distribution of the human chloride channel. CLC-5, reveals a pathophysiological basis for Dent's disease. *Hum Mol Genet* 8: 247–257, 1999
21. Morath R, Klein T, Seyberth HW, Nusing RM: Immunolocalization of the four prostaglandin E2 receptor proteins EP1, EP2, EP3, and EP4 in human kidney. *J Am Soc Nephrol* 10: 1851–1860, 1999
22. Raymond JR, Kim J, Beach RE, Tisher CC: Immunohistochemical mapping of cellular and subcellular distribution of 5-HT1A receptors in rat and human kidneys. *Am J Physiol* 264: 9–19, 1993
23. Foultier B, Troisfontaines P, Vertommen D, Marenne MN, Rider M, Parsot C, Cornelis GR: Identification of substrates and chaperone from the Yersinia enterocolitica 1B Ysa type III secretion system. *Infect Immun* 71: 242–253, 2003
24. Pennica D, Kohr WJ, Kuang WJ, Glaister D, Aggarwal BB, Chen EY, Goeddel DV: Identification of human uromodulin as the Tamm-Horsfall urinary glycoprotein. *Science* 236: 83–88, 1987
25. Rindler MJ, Naik SS, Li N, Hoops TC, Peraldi MN: Uromodulin (Tamm-Horsfall glycoprotein/uromucoid) is a phosphatidylinositol-linked membrane protein. *J Biol Chem* 265: 20784–20789, 1990
26. Jovine L, Qi H, Williams Z, Litscher E, Wassarman PM: The ZP domain is a conserved module for polymerization of extracellular proteins. *Nat Cell Biol* 4: 154–155, 2002
27. Brown D, Waneck GL: Glycosyl-phosphatidylinositol-anchored membrane proteins. *J Am Soc Nephrol* 3: 895–906, 1992
28. Kokot F, Dulawa J: Tamm-Horsfall protein updated. *Nephron* 85: 97–102, 2000
29. Auranen M, Ala-Mello S, Turunen JA, Jarvela I: Further evidence for linkage of autosomal-dominant medullary cystic kidney disease on chromosome 1q21. *Kidney Int* 60: 1225–1232, 2001
30. Fuchshuber A, Kroiss S, Karle S, Berthold S, Huck K, Burton C, Rahman N, Koptides M, Deltas C, Otto E, Ruschendorf F, Feest T, Hildebrandt F: Refinement of the gene locus for autosomal dominant medullary cystic kidney disease type 1 (MCKD1) and construction of a physical and partial transcriptional map of the region. *Genomics* 172: 278–284, 2001
31. Kroiss S, Huck K, Berthold S, Ruschendorf F, Scolari F, Caridi G, Ghiggeri GM, Hildebrandt F, Fuchshuber A: Evidence of further genetic heterogeneity in autosomal dominant medullary cystic kidney disease. *Nephrol Dial Transplant* 15: 818–821, 2000
32. Bingham C, Ellard S, van't Hoff WG, Simmonds HA, Marinaki AM, Badman MK, Winocour PH, Stride A, Lockwood CR, Nicholls AJ, Owen KR, Spyer G, Pearson ER, Hattersley AT: Atypical familial juvenile hyperuricemic nephropathy associated with a hepatocyte nuclear factor-1beta gene mutation. *Kidney Int* 63: 1645–1651, 2003
33. Ronco P, Brunisholz M, Geniteau-Legendre M, Chatelet F, Verroust P: Physiopathologic aspects of Tamm-Horsfall protein: A phylogenetically conserved marker of the thick ascending limb Henle's loop. *Adv Nephrol Necker Hosp* 16: 231–249, 1987
34. Fukuoka S, Freedman SD, Yu H, Sukhatme VP, Scheele GA: GP-2/THP gene family encodes self-binding glycosylphosphatidylinositol-anchored proteins in apical secretory compartments of pancreas and kidneys. *Proc Natl Acad Sci U S A* 89: 1189–1193, 1992
35. Lambert C, Brealey R, Steele J, Rook GA: The interaction of Tamm-Horsfall protein with the extracellular matrix. *Immunology* 79: 203–210, 1993
36. Stefanova I, Horejsi V, Ansotegui IJ, Knapp W, Stockinger H: GPI-anchored cell-surface molecules complexed to protein tyrosine kinases. *Science* 5034: 1016–1019, 1991
37. Thomas DB, Davies M, Williams JD: Tamm-Horsfall protein: An etiological agent in tubulointerstitial disease? *Exp Nephrol* 5: 281–284, 1993
38. Yu H, Papa F, Sukhatme VP: Bovine and rodent Tamm-Horsfall protein (THP) genes: Cloning structural analysis, and promoter identification. *Gene Expr* 4: 63–75, 1994
39. Hoops TC, Rindler MJ: Isolation of the cDNA encoding glycoprotein-2 (GP-2), the major zymogen granule membrane protein. Homology to uromodulin/Tamm-Horsfall protein. *J Biol Chem* 266: 4257–4263, 1991
40. Stenflo J, Stenberg Y, Muranyi A: Calcium-binding EGF-like modules in coagulation proteinases: Function of the calcium ion in module interactions. *Biochim Biophys Acta* 1477: 51–63, 2000
41. Collod-Beroud G, Beroud C, Ades L, Black C, Boxer M, Brocks DJH, Holman KJ, de Paepe A, Francke U, Grau U, Hayward C, Klein HG, Liu WG, Nuytinck L, Peltonen L, Perez ABA, Rantamaki T, Junien C, Boileau C: Marfan Database (third edition): New mutations and new routines for the software. *Nucleic Acids Res* 26: 229–233, 1998
42. Joutel A, Corpechot C, Ducros A, Vahedi K, Chabriat H, Mouton P, Alamowitch S, Domenga V, Cecillion M, Marechal E, Maciazek J, Vayssiere C, Cruaud C, Cabanis EA, Ruchoux MM, Weissenbach J, Bach JF, Bousser MG, Tournier-Lasserve E: Notch 3 mutations in CADASIL, a hereditary adult-onset condition causing stroke and dementia. *Nature* 383: 707–710, 1996
43. Whiteman P, Handford PA: Defective secretion of recombinant fragments of fibrillin-1: Implications of protein misfolding for the pathogenesis of Marfan syndrome and related disorders. *Hum Mol Genet* 12: 727–737, 2003
44. Sikri KL, Foster CL, MacHugh N, Marshall RD: Localization of Tamm-Horsfall glycoprotein in the human kidney using immuno-fluorescence and immuno-electron microscopical techniques. *J Anat* 132: 597–605, 1981
45. Lisanti MP, Sargiacomo M, Graeve L, Saltiel AR, Rodriguez-Boulan E: Polarized apical distribution of glycosyl-phosphatidylinositol-anchored proteins in a renal epithelial cell line. *Proc Natl Acad Sci U S A* 85: 9557–9561, 1988
46. Cavallone D, Malagolini N, Serafini-Cessi F: Mechanism of release of urinary Tamm-Horsfall glycoprotein from the kidney GPI-anchored counterpart. *Biochem Biophys Res Commun* 280: 110–114, 2001
47. Moro F, Ogg CS, Simmonds HA, Cameron JS, Chantler C, McBride MB, Duley JA, Davies PM: Familial juvenile gouty nephropathy with renal urate hypoexcretion preceding renal disease. *Clin Nephrol* 35: 263–269, 1991
48. McBride MB, Simmonds HA, Moro F: Familial renal disease or familial juvenile hyperuricaemic nephropathy? *J Inherit Metab Dis* 20: 351–353, 1997
49. Hoyer JR, Sisson SP, Vernier RL: Tamm-Horsfall glycoprotein: Ultrastructural immunoperoxidase localization in rat kidney. *Lab Invest* 41: 168–73, 1979
50. Sica DA, Schoolwerth AC: Renal handling of organic anions and cations and renal excretion of uric acid. In: The Kidney, 5th Ed., edited by Brenner BM, Philadelphia, WB Saunders, 1996, pp 607–700
51. Puig JG, Miranda ME, Mateos FA, Picazo ML, Jimenez ML, Calvin TS, Gil AA: Hereditary nephropathy associated with hyperuricemia and gout. *Arch Intern Med* 153: 357–365, 1993